Solid-State Nuclear Magnetic Resonance Analysis of the Conformation of an Inhibitor Bound to Thermolysin

Denise D. Beusen,*,† Lynda M. McDowell, Urzula Slomczynska,‡,§ and Jacob Schaefer

Center for Molecular Design and Departments of Pharmacology and Chemistry, Washington University, One Brookings Drive, St. Louis, Missouri 63130

Received February 9, 1995®

A number of structural experimental methods are available to determine the receptor-bound conformation of ligands as part of the process of rational drug design, including X-ray diffraction and solution-state NMR. Not all receptor/ligand systems are amenable to these types of analyses due to difficulties in sample preparation or inherent limitations of the methods. Rotational echo double-resonance (REDOR) NMR is a solid-state, magic angle-spinning technique that measures the dipolar coupling between specifically labeled nuclei and enables the determination of internuclear distance. In previous studies of helical peptides, we have verified the ability of REDOR NMR to measure distances accurately and precisely. In this study we use REDOR and double REDOR to measure distances between backbone atoms in a phosphonamidate transition-state inhibitor bound to thermolysin. The $^{31}P-^{13}C'$, $^{31}P-^{15}N$, and $^{31}P-^{13}C\alpha$ distances (3.61 ± 0.10, 3.89 ± 0.12, and 5.37 ± 0.13 Å, respectively) measured in a complex of Cbz-Gly^{P}-[1-^{13}C]Leu-[^{15}N,2-^{13}C]Ala and the enzyme are consistent with those observed by X-ray diffraction in other comparable thermolysin/inhibitor complexes (average values of 3.58 ± 0.04, 3.91 ± 0.13, and 5.17 ± 0.18 Å, respectively). These results demonstrate that REDOR NMR is a viable alternative to more traditional methods such as X-ray diffraction, transferred NOESY, and isotope-edited NOESY for characterizing the receptor-bound conformation of ligands.

Introduction

For flexible ligands which interact in a specific fashion with a receptor, it is generally accepted that biological activity is coupled to ligand conformation. Key functional groups of the ligand and the receptor must adopt a precise spatial orientation in order to elicit the activity of interest, whether it involves signal transduction at a protein receptor or catalysis to convert substrate to product. Consequently, the process of rationally designing ligands for receptors with potential as therapeutic agents can in principle be dramatically expedited by knowing the bound conformation of the ligand. A number of structural experimental methods[1] have been used to obtain this type of information: X-ray diffraction[2] and solution-state NMR methods such as transferred NOESY[3-5] and isotope-edited NOESY[6-10] are the most common. However, many receptor/ligand systems are not amenable to these types of analyses. Preparation of crystalline samples for X-ray analysis is not always straightforward, particularly for complexes which function within the cell membrane. Isotope-edited NOESY methods have effectively increased the molecular weight range accessible to solution NMR experiments by addressing the issue of spectral overlap, but the size of many interesting complexes results in dynamic properties incompatible with solution-NMR analysis.[6] Transferred NOESY methods can in principle sidestep this difficulty by virtue of looking only at the ligand, but this experiment is limited to ligands of relatively low affinity.[11]

In recent years, several solid-state NMR methods have been developed that supply structural information in situations where other methods are not practical.[12-16] Rotational echo double-resonance (REDOR) NMR is a solid-state, magic angle-spinning experiment that measures heteronuclear dipolar coupling between pairs of labeled nuclei and allows interatomic separation to be determined on the basis of the r^{-3} distance dependence of dipolar coupling.[17,18] We have previously demonstrated the ability of REDOR NMR to measure accurately interatomic distances in preparations of helical peptides.[19,20] REDOR NMR has been applied to a limited number of proteins and protein/ligand complexes for which X-ray or solution NMR information is unavailable.[14,21,22]

In our continuing efforts to demonstrate the versatility of REDOR as a method for generating structural information, we have measured internuclear distances in a specifically labeled inhibitor bound to thermolysin. This enzyme is a 34.6-kDa zinc endoproteinase from *Bacillus thermoproteolyticus*.[23] The metalloproteinases have diverse roles in regulating biological processes,[24] and several members of this family (angiotensin-converting enzyme,[25] matrix metalloproteinases,[26-28] and neutral endopeptidase[29]) have served as targets for drug-design efforts. As the first metalloproteinase to be characterized in atomic detail,[30] thermolysin has served an important role in comparative analyses designed to aid in understanding the mechanism and specificity of other zinc proteases and their inhibitors.[31-35] Several high-resolution structures of thermolysin bound to a variety of inhibitors are now available.[36,37] These include phosphoramidates[38] and phosphonamidates[39] which are presumed to be stable analogs of the tetrahedral transition state formed during peptide hydrolysis. In this study, we report REDOR measurements of

* Center for Molecular Design.
‡ Department of Pharmacology.
§ Current address: Receptor Laboratories, 2201 W. Campbell Park Dr., Chicago, IL 60612-3501. U.S. was on leave from the Institute of Organic Chemistry, Politechnika, Lodz, Poland.
® Abstract published in *Advance ACS Abstracts*, June 15, 1995.

0022-2623/95/1838-2742$09.00/0

internuclear distances in bound Cbz-Gly^P-[1-^{13}C]Leu-[^{15}N,2-^{13}C]Ala (ZG^{P}LA), a phosphonamidate transition-state analog inhibitor of thermolysin (K_i = 16.5 nM[40]). The superscript "P" indicates replacement of the planar carbonyl group by tetrahedral phosphorous. The observed ^{31}P–^{13}C and ^{31}P–^{15}N distances are in good agreement with crystallographic observations for these inhibitors and demonstrate the utility of REDOR NMR in providing structural information.

Experimental Methods

Materials. Thermolysin (~20% acetate salts) was purchased from Sigma. [1-^{13}C, 99%]Leu and [^{15}N,1-^{13}C, 99%]Ala were obtained from Cambridge Isotopes, Inc. Analytical HPLC was performed using a Vydac C_{18} column, 254 nm detection, flow rate of 1.0 mL/min, and solvents A (5% AcCN in 0.1 M H_2CO_3/Et_3N buffer, pH 7.5–7.6) and B (80% AcCN in 0.1 M H_2CO_3/Et_3N buffer, pH 7.5).

Synthesis of ZG^{P}LA. Methyl hydrogen [[*N*-(benzyloxycarbonyl)amino]methyl]phosphonate [Z-NH-CH_2-P(O)(OCH_3)-(OH)] was prepared as described previously by Jacobsen and Bartlett.[41] Boc-[1-^{13}C]Leu and [^{15}N,2-^{13}C]Ala-OMe were prepared from the respective free amino acids using standard methods[42,43] and coupled using isobutyl chloroformate in a mixed anhydride procedure.[43–45] The resulting Boc-[1-^{13}C]Leu-[^{15}N,2-^{13}C]Ala-OMe was treated with 1 N HCL/dioxane to yield HCl·[1-^{13}C]Leu-[^{15}N,2-^{13}C]Ala-OMe.

Z-NH-CH_2-P(O)(OCH_3)(OH) (0.259 g, 1.0 mmol) and triphenylphosphine (0.262 g, 1 mmol) in CCl_4:AcCN (1:1, 2 mL) were stirred at room temperature for 1.5 h. HCl·[1-^{13}C]Leu-[^{15}N,2-^{13}C]Ala-OMe (0.268 g, 1.0 mmol) and triethylamine (0.42 mL, 3 mmol) were added, and stirring was continued for 2 h. After evaporation to dryness, the residue was dissolved in chloroform and washed as a neutral product (10% H_2SO_4, water, 0.5 N $NaHCO_3$, water). After drying over $MgSO_4$, the solvent was evaporated and the crude product (Z-NH-CH_2-P(O)(OCH_3)-[1-^{13}C]Leu-[^{15}N,2-^{13}C]Ala-OMe) was purified by flash chromatography in CH_2Cl_2/MeOH (gradient from 98:2 to 96:4): yield 0.312 g (68%); R_f 0.158 (96:4 CH_2Cl_2/MeOH); analytical HPLC (gradient of 5–60% solvent B in 25 min) t_R 20.56, 21.28 min (two diastereomers), purity 99.3%.

Z-NH-CH_2-P(O)(OCH_3)-[1-^{13}C]Leu-[^{15}N,2-^{13}C]Ala-OMe (0.45 g, 0.1 mmol) was suspended in AcCN (0.2 mL), and 1.5 N LiOH (0.2 mL, 0.3 mmol) was added. After stirring at room temperature for 12 h, the mixture was lyophilized. The residue was dissolved in 2 mL of water and the pH adjusted to 8.5. The crude peptide was purifed by HPLC using a Vydac C_{18} column and a gradient of solvent B (5–60% in 40 min). The pure sample (30 mg, 63% yield) was dissolved in water and the pH adjusted to 8.5 with 1 N LiOH prior to a final lyophilization: analytical HPLC (gradient of 5–60% solvent B in 25 min) t_R 12.19 min, purity 99%. Solution ^{31}P and ^{1}H NMR were consistent with the previously reported product ZG^{P}LA (Z-NH-CH_2-P(O)(OLi)-Leu-Ala-OLi),[40] and FABMS revealed the incorporation of three additional mass units ($C_{16}{}^{13}C_2H_{26}N_2{}^{15}NO_7PLi_2$ *m*/*z* 445, MH^+).

Solid-State NMR Sample Preparation and Experimental Parameters. Thermolysin (346 mg, ~8 μmol) was dissolved in 600 μL of buffer (45% DMSO, v/v, 0.05 M Tris, pH 7.5, 2.5 M CsCl) and recrystallized by vapor diffusion against water as described previously.[30,46] After 3 weeks, crystals were recovered by centrifugation and resuspended in a solution of ZG^{P}LA (14.7 μmol) in 600 μL of buffer (7% DMSO, v/v, 0.01 M Tris, pH 7.3, 0.01 M $CaCl_2$). After 24–48 h, the suspension containing ~200 mg of crystalline protein was transferred to a 7-mm i.d. zirconia rotor for NMR experiments. The rotor was centrifuged, and excess inhibitor solution was removed by pipette. Kel-F endcaps and spacers were used to seal the rotor.

Experiments were performed on a home-built, four-channel spectrometer operating at 4.7 T (200 MHz for ^{1}H, 81 MHz for ^{31}P, 50 MHz for ^{13}C, and 20 MHz for ^{15}N NMR) which has been described previously.[19,47] Preliminary experiments at room temperature showed sample deterioration due to inductive heating. For data reported here, the sample was cooled through the use of an FTS compressor (to generate cooled air, −15 to −20 °C) and a Chemagnetics variable-temperature probe stack (to transfer the cold air to the probe). The sample temperature was approximately 10 °C. Cross-polarization transfers were performed at 38 kHz and proton decoupling at 80 kHz. Cross-polarization contact times were 1.0 ms for ^{31}P- and 2.0 ms for ^{13}C-observed experiments, and the recycle delay was 2.0 s. Sample spinning speeds of 4274 and 5000 Hz were used. Spectra were referenced to external standards (phosphocreatine for ^{31}P NMR and [4-^{13}C]Asn at 175.1 ppm for ^{13}C NMR) and processed with a line broadening of 20 Hz.

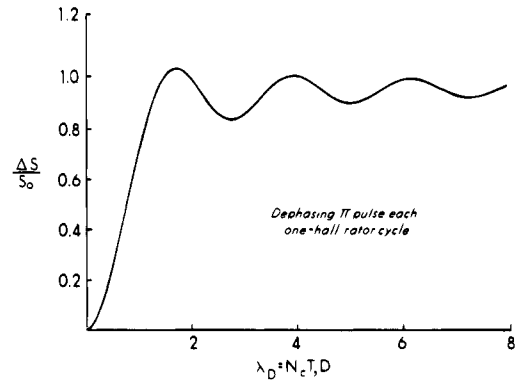

Figure 1. Theoretical curve showing the relationship between $\Delta S/S_0$ measured by REDOR and the dimensionless parameter λ_D. Because the number of rotor cycles for which the dephasing pulses are applied (N_c) and the rotor period (T_r = 1/spinning speed, in s) are known, determination of the dipolar coupling (D, in Hz) from the experimental $\Delta S/S_0$ is direct.

^{31}P-Observed, ^{15}N-Dephased REDOR. REDOR utilizes magic angle spinning and measures directly the heteronuclear dipolar coupling between isolated pairs of labeled nuclei. In a solid with ^{31}P–^{15}N dipolar coupling, the ^{31}P rotational spin echoes which form each rotor period following a ^{1}H–^{31}P cross-polarization transfer can be prevented from reaching full intensity by inserting rotor-synchronized π pulses on the ^{15}N channel. REDOR(xy-8) has π pulses on the observing channel (^{31}P) at the completion of each rotor period to refocus isotropic chemical shifts and π pulses on the other channel (^{15}N) at one-half the rotor period to dephase the transverse ^{31}P magnetization coupled to ^{15}N. The xy-8 phase-cycling scheme is used for both rare-spin channels.[14,22,48] The difference (ΔS) between the ^{31}P NMR spectrum obtained under these conditions (S) and the one obtained with no ^{15}N π pulses (S_0) depends on the strength of the dipolar coupling (D), the number of rotor cycles over which dephasing occurs (N_c), and the rotor period (T_r = 1/spinning speed).[18] The ratio $\Delta S/S_0$ was measured for several values of N_c to determine λ_D (see Figure 1) which specifies D. The interatomic distance, r, is calculated from the ^{31}P–^{15}N dipolar coupling using the well-known relationship $D = \gamma_N\gamma_P h/2\pi r^3$, where γ_N and γ_P are the gyromagnetic ratios of ^{15}N and ^{31}P, respectively, and h is Planck's constant. A small correction to r compensates for residual motion in the solid.[22] The low natural abundance contribution for ^{15}N meant that the dipolar coupling could be calculated directly from $\Delta S/S_0$ without any correction for background contribution. The total acquisition time for the REDOR data obtained by this method (summarized in Table 1) was 22.8 h.

^{13}C-Observed, ^{15}N-Dephased, ^{31}P-Dephased Double REDOR. A ^{13}C-observed, ^{31}P-dephased REDOR experiment analogous to the experiments described above could in principle yield the desired ^{13}C–^{31}P distances. However, natural abundance ^{13}C contributions to the full-echo signal are a potential source of error in measurement of these distances.[49] This limitation can be circumvented by incorporating a nearby ^{15}N and using it to select the ^{13}C signal(s) of interest.[19,47] In this study, we have elected to use double REDOR and the ^{15}N label between the two ^{13}C nuclei of interest to select their signal from the large background of ^{13}C resonances arising from natural abundance ^{13}C. In this double-REDOR application, two REDOR experiments are performed successively. The

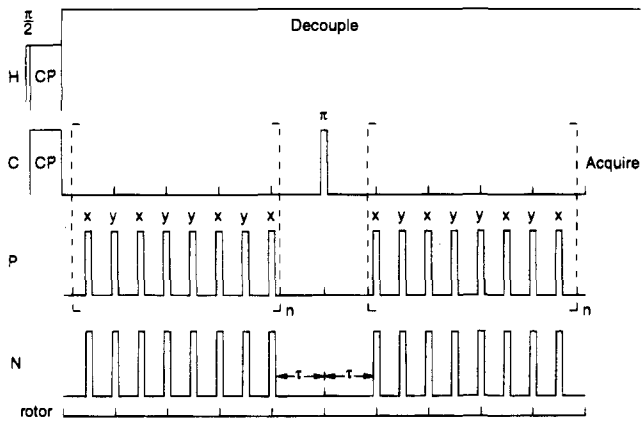

Figure 2. Double-REDOR pulse sequence. The data are collected as a set of two alternate-block experiments with the dephasing pulses turned off for the full-echo signal. Either ^{15}N or ^{31}P pulses are on for a given experiment. The dashed lines indicate a loop in the sequence with n being an integer loop counter whose smallest value ($n = 1$) corresponds to eight rotor cycles of ^{31}P-dephasing pulses. The ^{15}N dephasing is always eight rotor cycles and τ is $[4(n - 1) + 1]$ rotor periods. Thus, the ^{15}N-dephased and ^{31}P-dephased experiments have the same total evolution time and have full-echo signals with the same intensity. The xy-8 phase cycling of the π pulses minimizes errors due to pulse imperfections and was used for both ^{15}N-dephased and ^{31}P-dephased experiments. The central ^{13}C π pulse refocuses isotropic chemical shifts.

first experiment uses ^{15}N π pulses to dephase the ^{13}C signal and serves to select the ^{13}C signal of interest. Because the $^{15}N-^{13}C$ pair is so closely positioned (in this case directly bonded), their interaction dominates the $^{15}N-^{13}C$ dipolar coupling in the sample. The difference signal from this experiment defines S_0 for the specifically labeled ^{13}C atoms. In the second REDOR experiment, ^{31}P-dephasing pulses result in a difference signal, ΔS, from which the $^{13}C-^{31}P$ dipolar interaction can be calculated using S_0 as determined from the first experiment.

The double-REDOR experiment pulse sequence is shown in Figure 2. The presence of two nearby carbon-13 atoms with a large isotropic shift difference in the labeled ZG^{P}LA prohibits use of REDOR(xy-8) due to the SEDRA effect.[50] The single ^{13}C pulse in the center (Figure 2) adequately refocuses isotropic chemical shifts if the number of rotor cycles is not too large. Thus, this version of REDOR is acceptable when the dipolar coupling is reasonably strong (>50 Hz). The experiments were performed with (4274 Hz spinning speed) and without (5000 Hz spinning speed) CEDRA conditions[51] to prove the absence of SEDRA distortions in the signal intensities. Separate, interleaved experiments were run with either ^{31}P dephasing or ^{15}N dephasing. The dephasing pulses were turned off every other scan to collect the full-echo signal. Measurements were made with different numbers of rotor cycles of ^{31}P dephasing. The ^{15}N dephasing was always over 8 rotor periods, but τ was changed so the total evolution time was identical to that of the corresponding ^{31}P-dephase experiment. The total acquisition time for the REDOR data obtained by this method (summarized in Table 2) was 147.2 h.

Molecular Modeling. Coordinates for thermolysin/inhibitor complexes were obtained from the Brookhaven Protein Data Bank,[52] and coordinates for small molecules were retrieved from the Cambridge Structural Database.[53] Coordinates were imported into SYBYL[54] for measurement of internuclear distances.

Results and Discussion

^{31}P-Observed, ^{15}N-Dephased REDOR Distance Measurements. A ^{31}P REDOR spectrum of ZG^{P}LA complexed to thermolysin with $N_c = 24$ is shown in Figure 3. The full-echo spectrum (bottom) consists primarily of the bound form of the inhibitor at 31.6 ppm

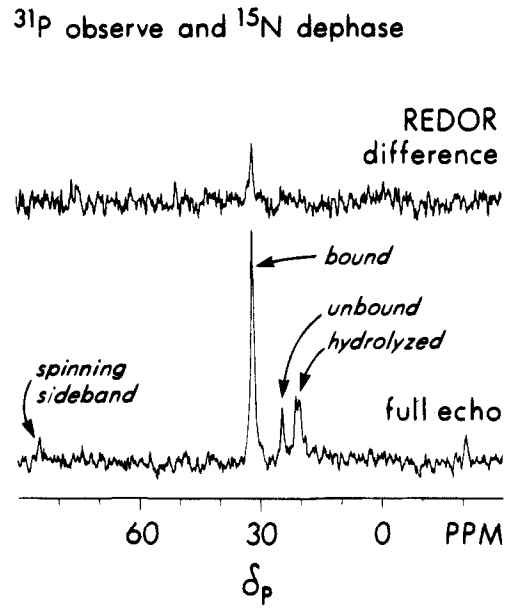

Figure 3. ^{31}P REDOR spectrum of ZG^{P}LA (Cbz-Gly^P-[1-^{13}C]-Leu-[^{15}N,2-^{13}C]Ala) complexed to thermolysin with 24 rotor cycles of ^{15}N dephasing. The full echo is shown at the bottom, with the ^{15}N-dephased REDOR difference spectrum shown above. The spinning speed was 4274 Hz.

Table 1. Summary of Distances Measured by REDOR NMR in ZG^{P}LA (Cbz-Gly^P-[1-^{13}C]Leu-[^{15}N,2-^{13}C]Ala) Complexed with Thermolysin

dephasing nucleus	observed nucleus	rotor cycles of dephasing	$\Delta S/S_0$	λ_D	REDOR distance (Å)
Ala N	P	16	0.09	0.30	3.98
		24	0.24	0.50	3.79
		32	0.34	0.61	3.89

with its associated spinning sidebands. In order to assign the observed peaks, a complex of ZG^{P}LA and thermolysin using a four-fold excess of inhibitor was prepared and solubilized using a previously reported protocol.[55] A solution ^{31}P NMR analysis (not shown) was comparable to previously reported solution spectra of ZG^{P}LA bound to thermolysin.[56] This study confirmed the identity of the bound inhibitor peak as well as a small peak at 24.4 ppm arising from unbound inhibitor and a doublet at 20/21 ppm arising from hydrolyzed inhibitor (Figure 3, bottom). Dephasing of the ^{31}P echo by ^{15}N yielded the difference spectrum (ΔS) shown in Figure 3 (top). Several ^{31}P-observed, ^{15}N-dephased REDOR measurements were made using different numbers of rotor cycles of dephasing, and the results are summarized in Table 1.

^{13}C-Observed, ^{15}N-Dephased, ^{31}P-Dephased Double-REDOR Distance Measurements. The ^{13}C full-echo spectrum of ZG^{P}LA complexed to thermolysin is shown in Figure 4 (bottom). Sharp, intense peaks at 48.6 and 175.9 ppm are consistent with the incorporated labels; however, the natural abundance contribution to the spectrum from the many carbon atoms in the complex is evident. The ^{13}C-observed, ^{15}N-dephased REDOR difference spectrum (Figure 4, middle) with $N_c = 8$ selects only the two specifically labeled carbon atoms and effectively eliminates the natural abundance background. Because the ^{15}N is directly bonded to both ^{13}C atoms, its dipolar coupling to these two atoms is strong and the REDOR difference maximizes ($\Delta S/S_0 \sim 1$) at a small number of rotor cycles of dephasing.[18] In

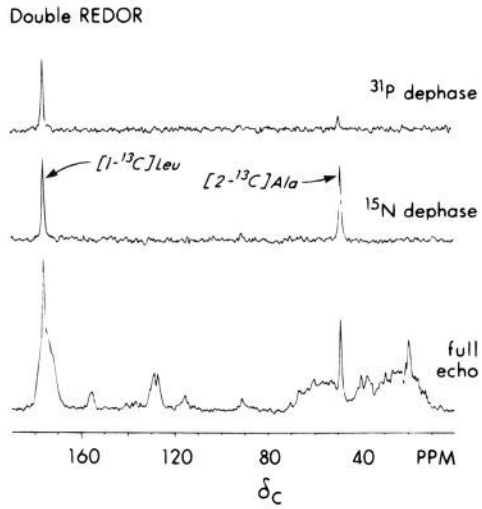

Figure 4. ^{13}C double-REDOR spectra of ZG^PLA (Cbz-Gly^P-[1-^{13}C]Leu-[^{15}N,2-^{13}C]Ala) complexed to thermolysin. Bottom: ^{13}C full-echo spectrum with 4274-Hz magic angle spinning. Middle: ^{13}C-Observed, ^{15}N-dephased REDOR difference spectrum, with eight rotor cycles of ^{15}N dephasing and 16 plus 2 rotor cycles with no dephasing (see caption of Figure 2). The strong dipolar coupling between the directly bonded $^{13}C-^{15}N$ pairs was used to select the specifically labeled carbons from the background of natural abundance ^{13}C. Top: ^{13}C-Observed, ^{31}P-dephased REDOR difference spectrum, $N_c = 24$. C−P dipolar couplings free from contributions due to natural abundance background were determined from $\Delta S/S_0$ where ΔS is the ^{13}C-observed, ^{31}P-dephased REDOR difference and S_0 is the ^{13}C-observed, ^{15}N-dephased REDOR difference.

Table 2. Summary of Distances Measured by Double-REDOR NMR in ZG^PLA (Cbz-Gly^P-[1-^{13}C]Leu-[^{15}N,2-^{13}C]Ala) Complexed with Thermolysin

dephasing nucleus	observed nucleus	rotor spinning speed[a] (Hz)	rotor cycles of dephasing	$\Delta S/S_0$	λ_D	REDOR distance (Å)
P	C′ of Leu	4274	8	0.24	0.50	3.54
		4274	16	0.61	0.89	3.68
P	Cα of Ala	4274	16	0.11	0.33	5.13
		4274	24	0.19	0.44	5.33
		4274	32	0.30	0.57	5.39
		4274	48	0.53	0.81	5.49
		5000	*24*	*0.13*	*0.36*	*5.41*
		5000	40	0.29	0.56	5.54
		5000	56	0.60	0.88	5.33

[a] Analyses at 4274 Hz were done under CEDRA conditions.

this case, background ^{13}C contributions to ΔS are negligible because they arise from weak (i.e., longer distance) dipolar couplings which have not evolved significantly for the small number of rotor cycles of dephasing used.

The ^{13}C-observed, ^{31}P-dephased REDOR difference spectrum (Figure 4, top) with $N_c = 24$ has significant intensity only from the specifically labeled carbon atoms. As natural abundance contributions to the full echo (Figure 4, bottom) can introduce errors in calculating C−P distances, the C−P dipolar couplings were determined using the ^{13}C-observed, ^{31}P-dephased REDOR difference for ΔS and the ^{13}C-observed, ^{15}N-dephased REDOR difference for S_0. Several ^{13}C-observed, ^{15}N-dephased, ^{31}P-dephased double-REDOR distance measurements were made using $N_c = 8$ for ^{15}N dephasing and a variable number of rotor cycles of ^{31}P dephasing. The results are summarized in Table 2.

Table 3. Intraligand Distances for Inhibitors Bound to Thermolysin Determined by X-ray Diffraction and Solid-State NMR

	X-ray (Å)					
atom pair	phosphor-amidon[a]	P-Leu-NH_2[a]	ZF^P-LA[b]	ZG^P-LL[b]	average	REDOR (Å) ZG^PLA[c]
P−R_1′C′	3.59	3.57	3.62	3.52	3.58 ± 0.04	3.61 ± 0.10
P−R_2′N	3.97	3.84	4.06	3.77	3.91 ± 0.13	3.89 ± 0.12
P−R_2′Cα	5.27	NA[d]	5.28	4.97	5.17 ± 0.18	5.37 ± 0.13

[a] Measured from X-ray coordinates reported in ref 38. [b] Measured from X-ray coordinates reported in ref 39. [c] Averaged values from Tables 1 and 2, measured by REDOR NMR. [d] NA, not applicable.

Comparison of REDOR-Measured Distances with Crystallographic Observations. Although no X-ray coordinates have been reported for ZG^PLA bound to thermolysin, a survey of the Brookhaven Protein Data Bank[52] revealed four relevant enzyme/inhibitor complexes having all or most of the atoms involved in the REDOR distance measurements. The inhibitors in these complexes are ZF^PLA (Cbz-Phe^P-Leu-Ala; 4TMN[39]), ZG^PLL (Cbz-Gly^P-Leu-Leu; 5TMN[39]), P-Leu-NH_2 (*N*-phosphorylleucinamide); 2TMN[38]), and phosphoramidon (*N*-(α-L-rhamnopyranosyloxyhydroxyphosphinyl)-Leu-Trp; 1TLP[38]). All are phosphorus-based, transition-state analog inhibitors of thermolysin in which the tetrahedral phosphorus mimics the tetrahedral intermediate formed at the scissile amide bond. In all four cases, Leu adjacent to the phosphorus binds in the S_1′ subsite, which is consistent with the known specificity of thermolysin.[57,58]

The structures of these four inhibitors when bound to thermolysin are shown in Figure 5. The structures have been overlaid and fit using the atoms involved in the REDOR analysis (P, R_1′C′, R_2′N, and R_2′Cα). The similarity of the backbone conformation in this region is evident. Interatomic distances in these structures corresponding to those measured by REDOR are summarized in Table 3. Notably, the bound conformation of the four inhibitors diverges only at the N-terminal side of the phosphorus center. In the case of ZF^PLA,

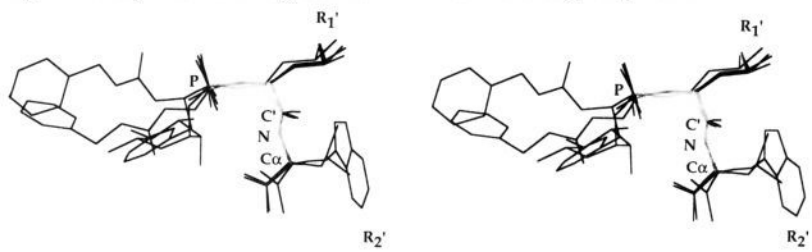

Figure 5. Crossed stereoview overlay of four phosphorylamide/phosphonamidate inhibitors bound to thermolysin as determined by X-ray diffraction. The four inhibitors are phosphorhamidon, P-Leu-NH_2, ZF^PLA, and ZG^PLL. The side chains which occupy the S_1′ and S_2′ binding pockets in thermolysin are indicated by R_1′ and R_2′. Coordinates were taken from the references listed in Table 3. The P, R_1′C′, R_2′N, and R′$_2$Cα atomic coordinates (corresponding to atoms involved in REDOR analyses) were aligned for best fit. Backbone atoms shared by the inhibitors are shown in gray.

the slow on-rate of the inhibitor has been linked to a conformation at the R_1 site that differs from that seen in ZG^{P}LL.[39,59] The inhibitor in this study (ZG^{P}LA) is kinetically similar to ZG^{P}LL in its rapid binding to the enzyme.[40]

Of the four X-ray structures, all but one (1TLP at 2.3 Å) have a reported resolution less than 2.0 Å. Careful examination of the structures reveals bond angles and bond lengths in the inhibitors that are not consistent with the expected ground-state structure. These deviations are possibly a consequence of the refinement protocol, in which covalent constraints involving the inhibitors were relaxed.[38,39] For example, P–N bond lengths in the ZF^{P}LA (1.899 Å) and P-Leu-NH_2 (1.849 Å) structures are significantly longer than the average value of 1.62 ± 0.03 Å observed in crystal structures of analogous small molecules (refcodes CRUFOM, DANHIJ, KEZTEO, PALPHS, PELRAZ, and TAFHIR in the Cambridge Structural Database[53]). It has been argued that Leu N is protonated in the bound inhibitor, thereby reducing the P–N double-bond character and elongating the P–N bond. Independent solid-state NMR measurements,[56] however, suggest that the P–N bond length for ZF^{P}LA and ZG^{P}LA is the same when bound to the enzyme and in solution and compares favorably (~1.65 Å) to the value cited above. In addition, the protonation state of Leu N in ZG^{P}LA and ZF^{P}LA does not change upon binding.[56] The size of the zinc coordination sphere varies among these inhibitors and is correlated with the reported P–N bond length. In P-Leu-NH_2 and ZF^{P}LA, both oxygens of the phosphorus moiety ligate to the pentacoordinate zinc. For phosphoramidon and ZG^{P}LL, only a single oxygen of the inhibitor is associated with the tetrahedral zinc. The different behavior is a consequence of rotation about the P–N bond.

As the bond angles and bond lengths which connect atoms in the backbone are significant factors in determining internuclear distances, a comparison of the internuclear distances measured by REDOR NMR in bound ZG^{P}LA to any one of the enzyme/inhibitor complexes may not be valid. In this case it is more appropriate to compare the distances measured by REDOR NMR to the *average* of the internuclear distances in all four reported enzyme/inhibitor complexes. In doing so, anomalies in the individual X-ray structures are smoothed. The internuclear distances determined by X-ray averaged over all four structures are reported in Table 3. Comparison of these values with the REDOR-measured distances reveals good agreement between the two methods.

Previous applications of REDOR NMR to biological samples have demonstrated the ability to measure accurately and precisely interatomic distances in pure preparations of peptides whose conformational state was known.[19,20] In this study, we have demonstrated the utility of REDOR NMR to provide similar high-quality structural data for a molecule bound to a receptor. Our results make it clear that REDOR NMR has the ability to provide information on the receptor-bound conformation of a ligand equivalent to that obtainable by solution-state NMR and X-ray methods. REDOR NMR, particularly because it can analyze complexes which are unapproachable by these more traditional methods, represents an addition to the repertoire of tools which can provide structural information essential to rational drug-design efforts.

Acknowledgment. The authors wish to thank Prof. F. Scott Matthews for useful discussions and Martin Gallagher for enzyme inhibition assays. Dimethyl phthaliminomethylphosphonate, an intermediate in the synthesis of Z-NH-CH_2-P(O)(OCH_3)(OH), was prepared by Dr. Jacek Koszuk at the Institute of Organic Chemistry, Politechnika, Lodz, Poland. This work was supported by grants to J. Schaefer (NIH GM-40634) and Garland Marshall (NIH GM-24483).

References

(1) Marshall, G. R.; Beusen, D. D.; Nikiforovich, G. V. Peptide Conformation-Stability and Dynamics. In *Peptides: Synthesis and Applications*; B. Gutte, Ed.; Academic Press: New York, in press.
(2) Whittle, P. J.; Blundell, T. L. Protein structure-based drug design. *Annu. Rev. Biophys. Biomol. Struct.* **1994**, *23*, 349–375.
(3) Campbell, A. P.; Van Eyk, J. E.; Hodges, R. S.; Sykes, B. D. Interaction of troponin I and troponin C: use of the two-dimensional transferred nuclear Overhauser effect to determine the structure of a Gly-110 inhibitory troponin I peptide analog when bound to cardiac troponin C. *Biochim. Biophys. Acta* **1992**, *1160*, 35–54.
(4) Ni, F.; Konishi, Y.; Scheraga, H. A. Thrombin-bound conformation of the C-terminal fragments of hirudin determined by transferred nuclear Overhauser effects. *Biochemistry* **1990**, *29*, 4479–4489.
(5) Sukumar, M.; Higashijima, T. G protein-bound conformation of mastoparan-X, a receptor-mimetic peptide. *J. Biol. Chem.* **1992**, *267*, 21421–21424.
(6) Wagner, G. Prospects for NMR of large proteins. *J. Biomol. NMR* **1993**, *3*, 375–385.
(7) Fesik, S. W. NMR studies of molecular complexes as a tool in drug design. *J. Med. Chem.* **1991**, *34*, 2937–2945.
(8) Fesik, S. W. NMR structure-based drug design. *J. Biomol. NMR* **1993**, *3*, 261–269.
(9) Fesik, S. W.; Gampe, R. T., Jr.; Eaton, H. L.; Gemmecker, G.; Olejniczak, E. T.; Neri, P.; Holzman, T. F.; Egan, D. A.; Edalji, R.; Simmer, R.; Helfrich, R.; Hochlowski, J.; Jackson, M. NMR Studies of [U-^{13}C] Cyclosporin A Bound to Cyclophilin: Bound Conformation and Portions of Cyclosporin Involved in Binding. *Biochemistry* **1991**, *30*, 6574–6583.
(10) Petros, A. M.; Kawai, M.; Luly, J. R.; Fesik, S. W. Conformation of two non-immunosuppressive FK506 analogs when bound to FKBP by isotope-filtered NMR. *FEBS Lett.* **1992**, *308*, 309–314.
(11) Clore, G. M.; Gronenborn, A. M. Theory and applications of the transferred nuclear Overhauser effect to the study of the conformations of small ligands bound to proteins. *J. Magn. Reson.* **1982**, *48*, 402–417.
(12) Bechinger, B.; Kim, Y.; Chirlian, L. E.; Gesell, J.; Neumann, J. M.; Montal, M.; Tomich, J.; Zasloff, M.; Opella, S. J. Orientations of amphipathic helical peptides in membrane bilayers determined by solid-state NMR spectroscopy. *J. Biomol. NMR* **1991**, *1*, 167–173.
(13) Beusen, D. D.; McDowell, L. M.; Schmidt, A.; Cohen, E. R.; Schaefer, J. Solid-state NMR determination of the geometry of substrate and inhibitor bound to EPSP synthase. In *Peptides: Chemistry, Structure, and Biology*; Hodges, R. S., Smith, J., Eds.; ESCOM: Leiden, The Netherlands, **1994**; pp 760–762.
(14) Christensen, A. M.; Schaefer, J. Solid-state NMR determination of intra- and intermolecular ^{31}P-^{13}C distances for shikimate 3-phosphate and [1-^{13}C]glyphosate bound to enolpyruvylshikimate-3-phosphate synthase. *Biochemistry* **1993**, *32*, 2868–2873.
(15) Ketchem, R. R.; Hu, W.; Cross, T. A. High-resolution conformation of gramicidin A in a lipid bilayer by solid-state NMR. *Science* **1993**, *261*, 1457–1460.
(16) McDermott, A. E.; Creuzet, F.; Gebhard, R.; van der Hoef, K.; Levitt, M. H.; Herzfeld, J.; Lugtenburg, J.; Griffin, R. G. Determination of internuclear distances and the orientation of functional groups by solid-state NMR: rotational resonance study of the conformation of retinal in bacteriorhodopsin. *Biochemistry* **1994**, *33*, 6129–6136.
(17) Gullion, T.; Schaefer, J. Rotational-Echo Double-Resonance NMR. *J. Magn. Reson.* **1989**, *81*, 196–200.
(18) Pan, Y.; Gullion, T.; Schaefer, J. Determination of C-N internuclear distances by rotational-echo double-resonance NMR of solids. *J. Magn. Reson.* **1990**, *90*, 330–340.
(19) Holl, S. M.; Marshall, G. R.; Beusen, D. D.; Kociolek, K.; Redlinski, A. S.; Leplawy, M. T.; McKay, R. A.; Vega, S.; Schaefer, J. Determination of an 8-Å interatomic distance in a helical peptide by solid-state NMR spectroscopy. *J. Am. Chem. Soc.* **1992**, *114*, 4830–4833.

(20) Marshall, G. R.; Beusen, D. D.; Kociolek, K.; Redlinski, A. S.; Leplawy, M. T.; Pan, Y.; Schaefer, J. Determination of a precise interatomic distance in a helical peptide by REDOR NMR. *J. Am. Chem. Soc.* **1990**, *112*, 963–966.
(21) Hing, A. W.; Tjandra, N.; Cottam, P. F.; Schaefer, J.; Ho, C. An investigation of the ligand-binding site of the glutamine-binding protein of *Escherichia coli* using rotational-echo double-resonance NMR. *Biochemistry* **1994**, *33*, 8651–8661.
(22) McDowell, L. M.; Holl, S. M.; Qian, S.-J.; Li, E.; Schaefer, J. Inter-tryptophan distances in rat cellular retinol binding protein II by solid-state NMR. *Biochemistry* **1993**, *32*, 4560–4563.
(23) Endo, S. The protease produced by thermophilic bacteria. *Hakko Kogaku Zasshi* **1962**, *40*, 346–353.
(24) Lennarz, W. J.; Strittmatter, W. J. Cellular functions of metalloendoproteinases. *Biochim. Biophys. Acta* **1991**, *1071*, 149–158.
(25) Wyvratt, M. J.; Patchett, A. A. Recent developments in the design of angiotensin-converting enzyme inhibitors. *Med. Res. Rev.* **1985**, *5*, 483–531.
(26) Brown, F. K.; Brown, P. J.; Bickett, D. M.; Chambers, C. L.; Davies, H. G.; Deaton, D. N.; Drewry, D.; Foley, M.; McElroy, A. B.; Gregson, M.; McGeehan, G. M.; Myers, P. L.; Norton, D.; Salovich, J. M.; Schoenen, F. J.; Ward, P. Matrix metalloproteinase inhibitors containing a (carboxyalkyl)amino zinc ligand: Modification of the P_1 and P_2' residues. *J. Med. Chem.* **1994**, *37*, 674–688.
(27) Gordon, J. L.; Drummond, A. H.; Galloway, W. A. Metalloproteinase inhibitors as therapeutics. *Clin. Exp. Rheum.* **1993**, *11* (Suppl. 8), S91–S94.
(28) Johnson, W. H.; Roberts, N. A.; Borkakoti, N. Collagenase inhibitors: their design and potential therapeutic use. *J. Enzyme Inhib.* **1987**, *2*, 1–22.
(29) Roques, B. P. Zinc metallopeptidases: active site structure and design of selective and mixed inhibitors: New approaches in the search for analgesics and anti-hypertensives. *Biochem. Soc. Trans.* **1993**, *21*, 678–685.
(30) Matthews, B. W.; Jansonius, J. N.; Colman, P. M.; Schoenborn, B. P.; Dupourque, D. Three-dimensional structure of thermolysin. *Nature (London), New Biol.* **1972**, *238*, 37–40.
(31) Rich, D. H. Peptidase inhibitors. In *Enzymes and other molecular targets*; Sammes, P. G., Ed.; Pergammon Press: New York, 1990; Vol. 2; pp 391–441.
(32) Vallee, B. L.; Auld, D. S. Active-site zinc ligands and activated H_2O of zinc enzymes. *Proc. Natl. Acad. Sci. U.S.A.* **1990**, *87*, 220–224.
(33) Jiang, W.; Bond, J. S. Families of metalloendopeptidases and their relationships. *FEBS Lett.* **1992**, *312*, 110–114.
(34) Monzingo, A. F.; Matthews, B. W. Structure of a mercaptan-thermolysin complex illustrates mode of inhibition of zinc proteases by substrate-analogue mercaptans. *Biochemistry* **1982**, *21*, 3390–3394.
(35) Monzingo, A. F.; Matthews, B. W. Binding of N-carboxymethyl dipeptide inhibitors to thermolysin determined by X-ray crystallography: A novel class of transition-state analogues for zinc peptidases. *Biochemistry* **1984**, *23*, 5724–5729.
(36) Matthews, B. W. Structural basis of the action of thermolysin and related zinc peptidases. *Acc. Chem. Res.* **1988**, *21*, 333–340.
(37) Tronrud, D. E.; Roderick, S. L.; Matthews, B. W. Structural basis for the action of thermolysin. *MATRIX Suppl.* **1992**, *1*, 107–111.
(38) Tronrud, D. E.; Monzingo, A. F.; Matthews, B. W. Crystallographic structural analysis of phosphoramidates as inhibitors and transition-state analogs of thermolysin. *Eur. J. Biochem.* **1986**, *157*, 261–268.
(39) Holden, H. M.; Tronrud, D. E.; Monzingo, A. F.; Weaver, L. H.; Matthews, B. W. Slow- and fast-binding inhibitors of thermolysin display different modes of binding: Crystallographic analysis of extended phosphonamidate transition-state analogues. *Biochemistry* **1987**, *26*, 8542–8553.
(40) Bartlett, P. A.; Marlowe, C. K. Phosphonamidates as transition-state analogue inhibitors of thermolysin. *Biochemistry* **1983**, *22*, 4618–4624.
(41) Jacobsen, N. E.; Bartlett, P. A. A phosphonamidate dipeptide analogue as an inhibitor of Carboxypeptidase A. *J. Am. Chem. Soc.* **1981**, *103*, 654–657.
(42) Fisher, E. On the esters of amino acids. *Ber. Deutsch. Chem. Ges.* **1901**, *34*, 433–454.
(43) Bodansky, M.; Bodansky, A. *The practice of peptide synthesis*, 2nd ed.; Springer-Verlag: Berlin, 1994.
(44) Vaughan, J. R., Jr. Acylalkylcarbonates as acylating agents *J. Am. Chem. Soc.* **1951**, *73*, 3547.
(45) Vaughan, J. R., Jr.; Osato, R. L. The preparation of peptides using mixed carbonic-carboxylic acid anhydrides. *J. Am. Chem. Soc.* **1952**, *74*, 676–678.
(46) Holmes, M. A.; Matthews, B. W. Structure of thermolysin refined at 1.6Å resolution. *J. Mol. Biol.* **1982**, *160*, 623–639.
(47) Holl, S. M.; McKay, R. A.; Gullion, T.; Schaefer, J. Rotational-echo triple-resonance NMR. *J. Magn. Reson.* **1990**, *89*, 620–626.
(48) Gullion, T.; Baker, D. B.; Conradi, M. S. New, compensated Carr-Purcell sequences. *J. Magn. Reson.* **1990**, *89*, 479–484.
(49) Hing, A. W.; Vega, S.; Schaefer, J. Measurement of heteronuclear dipolar coupling by transferred-echo double-resonance NMR. *J. Magn. Reson. Ser. A* **1993**, *103*, 151–162.
(50) Gullion, T.; Vega, S. A simple magic angle spinning NMR experiment for the dephasing of rotational echoes of dipolar-coupled homonuclear spin pairs. *Chem. Phys. Lett.* **1992**, *194*, 423–428.
(51) Zhu, W.; Klug, C. A.; Schaefer, J. Measurement of dipolar coupling within isolated spin-1/2 homonuclear pairs by CEDRA NMR. *J. Magn. Reson. Ser. A* **1994**, *108*, 121–123.
(52) Protein Data Bank Chemistry Department, Bldg. 555, Brookhaven National Laboratory, P.O. Box 5000, Upton, NY 11973–5000.
(53) Cambridge Structural Database System 3, Cambridge Crystallographic Data Center, 12 Union Rd., Cambridge CB2 1EZ, United Kingdom.
(54) SYBYL 6.03, Tripos Assoc., Inc., 1699 S. Hanley Rd., Suite 303, St. Louis, MO 63144.
(55) Gettins, P. Thermolysin-inhibitor complexes examined by ^{31}P and ^{113}Cd NMR spectroscopy. *J. Biol. Chem.* **1988**, *263*, 10208–10211.
(56) Copie, V.; Kolbert, A. C.; Drewry, D. H.; Bartlett, P. A.; Oas, T. G.; Griffin, R. G. Inhibition of thermolysin by phosphonamidate transition-state analogues: measurement of ^{31}P-^{15}N bond lengths and chemical shifts in two enzyme-inhibitor complexes by solid-state nuclear magnetic resonance. *Biochemistry* **1990**, *29*, 9176–9184.
(57) Matsubara, H.; Sasaki, R.; Singer, A.; Jukes, T. H. Specific nature of hydrolysis of insulin and tobacco mosaic virus protein by thermolysin. *Arch. Biochem. Biophys.* **1966**, *115*, 324–331.
(58) Morihara, K.; Tsuzuki, H.; Oka, T. Comparison of the specificities of various neutral proteases from microorganisms. *Arch. Biochem. Biophys.* **1968**, *123*, 572–588.
(59) Bartlett, P. A.; Marlowe, C. K. Possible role for water dissociation in the slow binding of phosphorus-containing transition-state-analogue inhibitors of thermolysin. *Biochemistry* **1987**, *26*, 8553–8561.

JM950101L